Characteristics of the SAR Distributions in a Head Exposed to Electromagnetic Fields Radiated by a Hand-Held Portable Radio

So-ichi Watanabe, *Student Member, IEEE*, Masao Taki, Toshio Nojima, *Member, IEEE*, and Osamu Fujiwara, *Member, IEEE*

Abstract— **This paper presents characteristics of the specific absorption rate (SAR) distributions calculated by the finite-difference time-domain (FDTD) method using a heterogeneous and realistic head model and a realistic hand-held portable radio model. The difference between the SAR distributions produced by a 1/4-wavelength monopole antenna and those produced by a 1/2-wavelength dipole antenna is investigated. The dependence of the maximum local SAR on the distance d_a between the auricle of the head and the antenna of the radio is evaluated. It is shown that the maximum local SAR decreases as the antenna length extends from 1/4 to 1/2 of the wavelength. The maximum local SAR's in a head model with auricles are larger than those in one without auricles. The dependence of the SAR on the electrical inhomogeneity of the tissues in the head model is not significant with regard to the surface distribution and the maximum local SAR when the radio is near the head. It is also shown that the maximum local SAR is not strongly dependent on the position of the hand when the hand does not shade the antenna. Furthermore, the SAR's experimentally measured in a homogeneous head phantom are compared with the calculated SAR's.**

I. Introduction

THE RECENT development of mobile communications has drawn attention to the biological effects of electromagnetic fields (EMF's). Apart from the controversy over the possible health hazards due to so-called nonthermal effect of EMF's, the electromagnetic interaction of a portable radio with a human head should be quantitatively evaluated in order to establish the safety of wireless communications. Specific absorption rate (SAR) has been recognized as one of the most significant variables quantifying the EMF interaction with the human body, and safety guidelines recommend limits on the maximum local SAR as well as on the whole-body averaged SAR [1], [2]. Evaluation of the maximum local SAR is especially important when part of the body is exposed to electromagnetic radiation from nearby sources. Thus the estimation of SAR distributions in a human head during the use of cellular telephones has become a matter of great concern.

The SAR distributions in a head exposed to EMF's from hand-held portable radios have been estimated through both experimental measurements [3]–[9] and numerical calculations [10]–[14]. Recent progress in the computer technology enables us to use the finite-difference time-domain (FDTD) method to numerically calculate the electromagnetic interactions of a heterogeneous, realistic head model with a realistic portable radio model. Dimbylow *et al.* [10], [11], for example, reported the SAR distribution and the dependence of the maximum local SAR on the distance between the head and the radio. Gandhi [13] presented the maximum local SAR's in the head exposed to EMF's from several types of radio models. These results have enhanced our comprehension of the interactions of a portable radio with a human head, but these interactions depend on various exposure conditions such as the antenna type, the electrical constants of tissues, the geometry of the head model, and the position of the hand holding the device. We therefore investigate the characteristics of power absorption in human head irradiated by EMF's from portable radios under various exposure conditions.

Portable radios with different types of antennas cause different interactions with a human head [12]. Most numerical studies using a realistic model of a portable radio, however, have assumed a 1/4-wavelength monopole antenna on the upper plane of the radio [11], [12], [14], [15]. But because a longer whip antenna such as a 3/8-wavelength or 1/2-wavelength antenna is also used in commercial portable radios [16], this paper presents the effects of antenna length on the SAR distributions.

In the ordinary use of hand-held portable radios, the maximum local SAR appears around the auricle close to the radio [13], and this implies that the maximum local SAR is significantly affected by the auricle. In most of previous studies, however, the auricles of the head were not modeled precisely [7], [8], [12], [15], [17]. This paper therefore investigates the effect of the auricle on the maximum local SAR.

A homogeneous phantom has been used in the experimental estimation of the SAR distribution in a head [3]–[5], [7], [8]. The human head is, however, inhomogeneous, and the effect of inhomogeneity in tissue electrical constants should be examined in order to evaluate the validity of experimental estimation of SAR's using a homogeneous head model. This paper therefore also investigates the effect of the inhomogeneity of head models on the SAR distributions and the maximum local SAR's.

A hand-held portable radio is usually supported by a hand when it is in use, and a previous study [12] has shown that

Manuscript received October 25, 1995; revised February 16, 1996.

S. Watanabe and M. Taki are with the Department of Electronics and Information Engineering, Tokyo MetropolitanUniversity, Tokyo 192-03, Japan.

T Nojima is with NTT Mobile Communications Network Inc., Yokosuka, 238-03, Japan.

O. Fujiwara is with the Faculty of Engineering, Nagoya Institute of Technology, Nagoya, 466, Japan.

Publisher Item Identifier S 0018-9480(96)07033-0.

TABLE I
THE ELECTRICAL PROPERTIES OF THE TISSUES IN THE HEAD MODEL AND OF THE DRY PHANTOM

	Frequency	Bone	Brain	Muscle	Eyeball	Fat	Skin	Lens	Phantom
Relative permittivity	900 MHz	9.67†	52.7†	59.1†	80.0‡	4.67†	59.1*	59.1*	52.0‡†
	1.5 GHz	7.75†	46.0†	55.3†	80.0‡	9.70‡‡	45.6‡‡	55.3*	38.0‡†
Conductivity [S/m]**	900 MHz	0.0508	1.05	1.26	1.90	0.0583	1.26	1.26	1.45
	1.5 GHz	0.105	1.65	2.00	1.90	0.270	1.93	2.00	1.17

†[19], ‡[20], ‡†[8], ‡‡[21]. *The values of muscle are used. **Their sources are the same as those of relative permittivity.

the hand which holds the portable radio significantly affects the antenna characteristics. The hand holding the radio should therefore affect the SAR distribution in the head, so this paper investigates the effect of the hand on the maximum local SAR's in the head.

The FDTD method is used in these investigations, and a heterogeneous, realistic model of a human head and a realistic model of a hand-held portable radio are assumed. The SAR distributions in a homogeneous head phantom exposed to EMF's from several prototypes of commercial hand-held portable radios are also measured experimentally by using the thermograph method, and those distributions are compared with the calculated ones.

II. CALCULATION MODEL AND METHOD

A. Head and Radio Models

The heterogeneous and realistic head model used in our calculations was based on an anatomical chart of a Japanese adult head [18]. The head model comprised 273 108 cubical cells 2.5 mm on a side.

The tissues constituting the head model were muscle, bone, skin, brain, fat, eyeball, and lens. The tissue electrical properties [19]–[21] are listed in Table I. The mass density of each of tissues was assumed to be 1000 kg/m^3. A horizontal section through the eyes of the head model and a midsagittal vertical section are shown in Fig. 1.

Since the hand-held portable radios in this study are operated at 900 MHz or at 1.5 GHz, the wavelengths of the EMF's which they produce are much shorter than the whole human body. It is therefore assumed that the body below the head does not affect the SAR distribution in the head when the radio is located in the vicinity of the head. This assumption has also been made in previous studies [10]–[12], [14], [15], and to examine its validity the SAR distribution in an isolated head model was compared with that in a whole-body model when both models were exposed to the near field of a short electric dipole at 300 MHz [22]. Both models comprised 1 × 1 × 1-cm cubical cells. The SAR distributions in these models were calculated with the FDTD method, and the distribution on the surface of the isolated head model agreed well with that of the whole-body model: the difference of the maximum local SAR's on the surface was within 2%. Although the difference between the local SAR's calculated with these models were as much as 37% in the deep region of the head, the absorption in the deep region is much smaller than the surface absorption and is not significant when compared with it. Moreover the difference at 900 MHz or 1.5 GHz is expected to be much smaller than that at 300 MHz. The isolated head model was thus used in the following calculations.

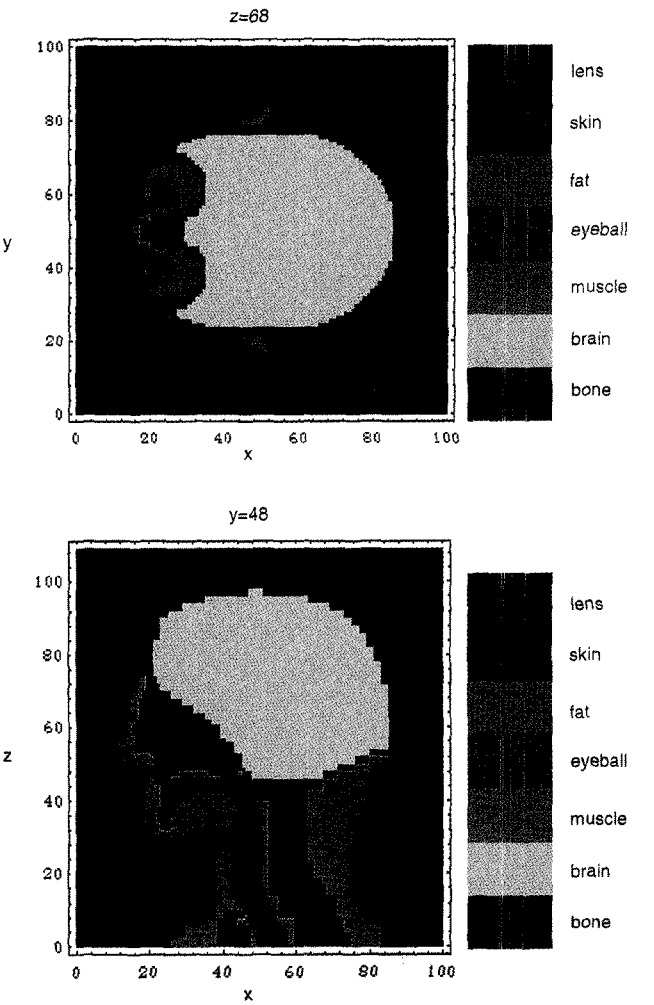

Fig. 1. The heterogeneous, realistic head model for FDTD calculation. The upper and lower drawings are, respectively, a horizontal section through the eyes and a midsagittal verticle section.

To investigate the effect of the electrical inhomogeneity of the head model, we also calculated the SAR distributions in a homogeneous head model whose shape was the same as that of the heterogeneous model. The electrical constants of the homogeneous model were assumed as those of the homogeneous head phantom used for the experimental measurement of the SAR distribution in this study.

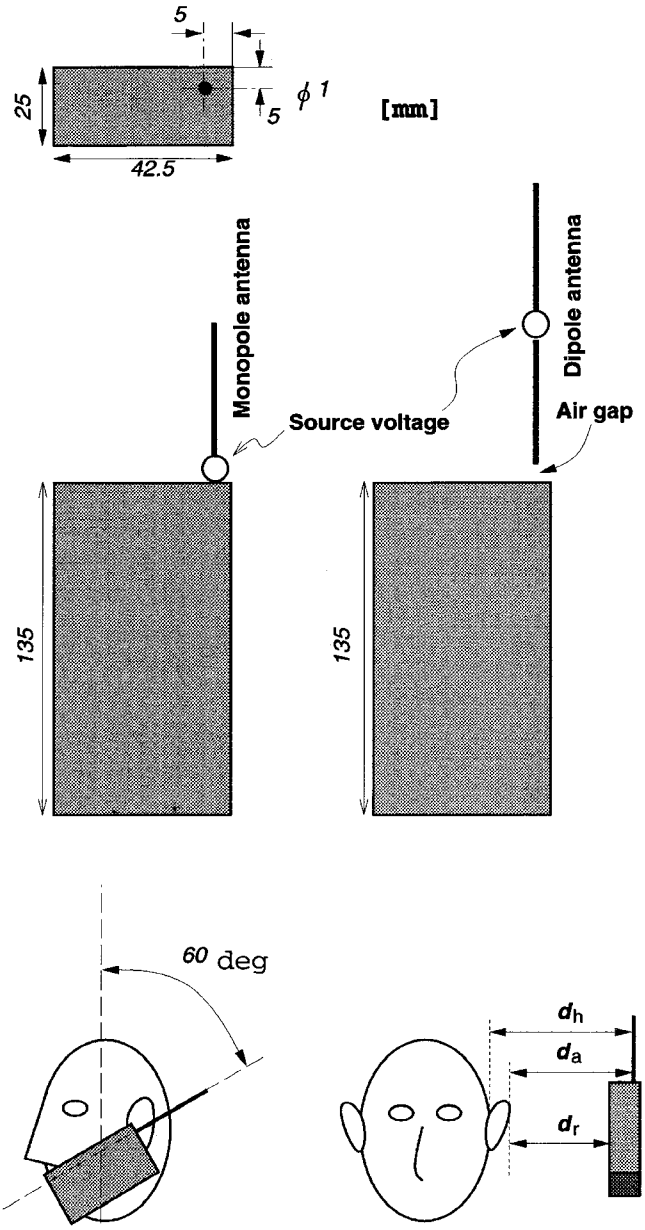

Fig. 2. Portable radio models and their position relative to the head.

The hand-held portable radio was assumed to be a 135 × 42.5 × 25-mm conducting box with either a 1/2-wavelength dipole antenna or a 1/4-wavelength monopole antenna on its upper plane. It was located on the left side of the head. To allow more realistic geometric relation between the head and a radio during ordinary use, the head model was rotated by 60° so that the radio model was positioned between the operator's mouth and ear. The dimension and the geometry of the radio model are shown in Fig. 2.

In previous studies, a radio model had not been supported with a hand, or a simple parallelepiped hand model holding a radio model had been assumed [11], [12], [15]. In this work therefore we have attempted to simulate the typical way in which a radio is held shown in Fig. 3 with 2 cm of space between the palm and the radio and with the thumb crooked around the radio.

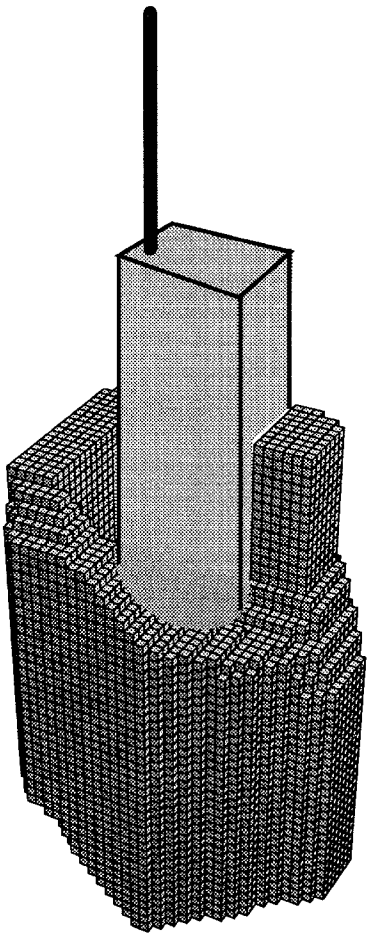

Fig. 3. Model of the hand holding the radio.

B. Calculation Method

The FDTD method [23]–[25] was used in calculating the SAR distributions in the head model. The following are the parameters of the FDTD calculation employed in this study. The cell size δ was 2.5 mm. The time step δ_t of the FDTD calculation was 4.17 ps ($\delta/2c_0$, where c_0 is the speed of light). The size of the calculation region was varied from 200 × 200 × 200 cells to 200 × 240 × 200 cells, as the distance between the surface of the portable radio model and the left auricle increased from 0 to 10 cm. The FDTD calculations were performed for 10 sinusoidal cycles to reach the steady state.

The second approximations of the absorbing boundary conditions [26] were assumed on the boundaries of the calculation region. Both antenna wire and handset were modeled by setting the electric fields, tangential to the surface, to zero (perfect conductor). The source voltage applied in the feed was a sinusoidal wave. Faraday's law was used in calculating the circumferential magnetic field strength adjacent to the antenna [27]. The current on the antenna wire was calculated by applying Ampere's law to the circumferential magnetic fields.

III. Experiment Model and Method

To compare the calculated results with measured results, we also obtained the SAR distributions on the surface of a

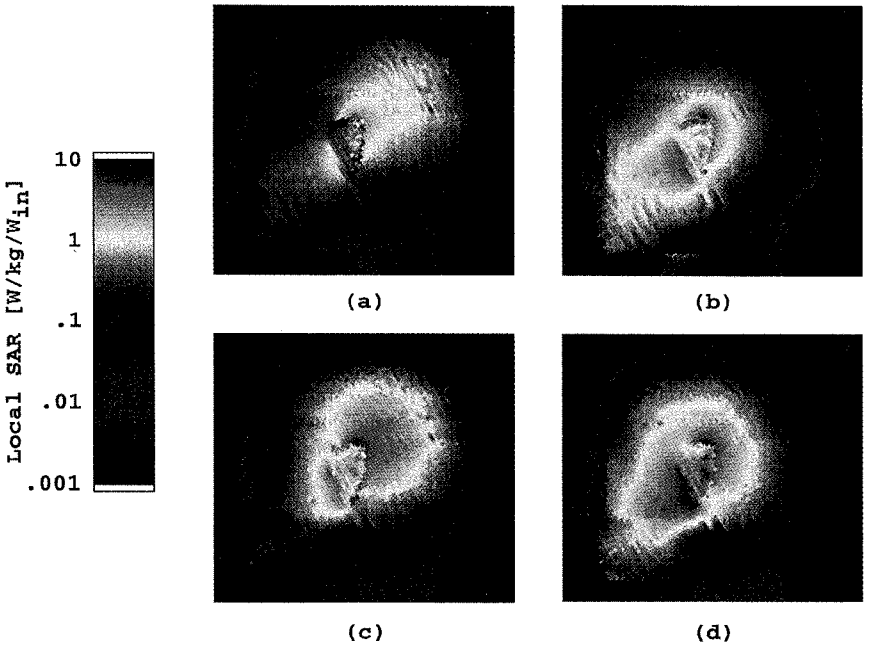

Fig. 4. The calculated SAR distributions on the surface of the heterogeneous head model exposed to EMF's from the portable radios. The antenna input power is 1 W, and the distance $\mathbf{d}_r$ between the surface of the radio and the auricle is 1 cm (i.e., $\mathbf{d}_a = 3$ cm). (a) 900-MHz 1/2-wavelength dipole. (b) 900-MHz 1/4-wavelength monopole. (c) 1.5-GHz 1/2-wavelength dipole. (d) 1.5-GHz 1/4-wavelength monopole.

homogeneous dry phantom of a human head experimentally. The SAR's were derived from the distributions of thermographically measured increases in temperature. The procedure and the setup of the experiment, as well as the validity of the SAR estimation using our thermography system, have been described in [7], [8].

The medium of the dry phantom was a homogeneous composite material consisting of ceramic powder, graphite powder, and bounding resin [7], [8]. Its electrical properties are listed in Table I. It should be noted that the shape of the head phantom is not exactly the same as that of the numerical head model, especially the shape of ears. That is, the auricles of the experimental head model are smaller in size and do not protrude markedly, while those of the numerical head model protrude 1.75 cm from the surface of the head.

Four types of hand-held portable radios with a whip antenna were examined. These were prototype commercial radio devices and were not the same as the model used in the calculations. The antenna lengths and the excitation frequencies of these radios are listed in Table II. The reflection powers of these radios were below -20 dB of the input power. Note that the antenna position relative to the upper plane of the radio varies with the type of the radio.

TABLE II
THE LENGTHS OF THE ANTENNAS AND THE EXCITATION FREQUENCIES OF THE PORTABLE RADIOS USED IN THE EXPERIMENT

Model	Frequency [MHz]	Antenna length [mm]	per wavelength
Radio A	934	115	0.358
Radio B	945	105	0.331
Radio C	940	100	0.313
Radio D	920	80	0.245

IV. RESULTS AND DISCUSSION

A. Effects of Antenna Type—SAR Distribution

Distribution on the Surface: The calculated SAR distributions on the surface of the heterogeneous head model irradiated by EMF's from the hand-held portable radios mounting the 1/2-wavelength dipole and the 1/4-wavelength monopole are shown in Fig. 4. The antenna input power is 1 W. The distance $\mathbf{d}_r$ between the left auricle of the head model and the surface of the conducting box of the radio model is 1 cm, which is a typical location of the radio in ordinary use. It should be noted that the axis of the antenna wire is 2 cm behind the surface of the radio model, and that the distance between the rim of the auricle and the surface of the head is 1.75 cm. Thus the distance $\mathbf{d}_a$ between the antenna and the auricle is 3 cm and the distance $\mathbf{d}_h$ between the antenna and the surface of the head is 4.75 cm. The hand holding the radio was not considered here.

During exposure to the EMF from the 1/2-wavelength dipole [Fig. 4(a) and (c)], a large amount of power is absorbed in the occipitotemporal area and in the area behind the auricle. With the exposure by the 1/4-wavelength monopole [Fig. 4(b) and (d)], on the other hand, the large SAR appears in the cheek and in the area behind the auricle. This implies that the SAR distribution on the surface of the head is strongly affected by the current distribution on the antenna and the conducting box of the radio.

Distribution in the Horizontal Section: The calculated SAR distributions in the horizontal section through the eyes of the heterogeneous head model are shown in Fig. 5. The exposure conditions in Fig. 5(a)–(d) are the same as those in

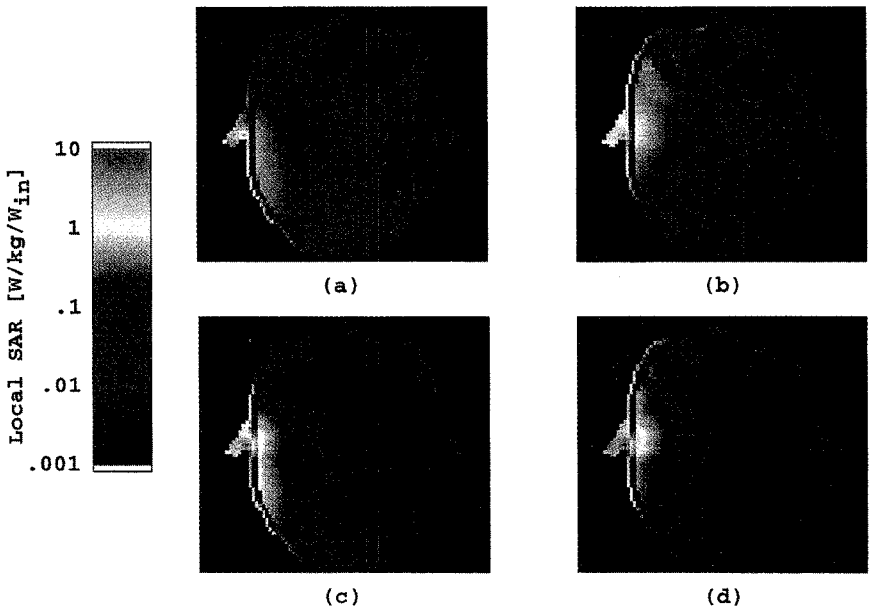

Fig. 5. The calculated SAR distributions in the horizontal section through the eyes of the heterogeneous head model. The exposure conditions are the same as those in Fig. 4.

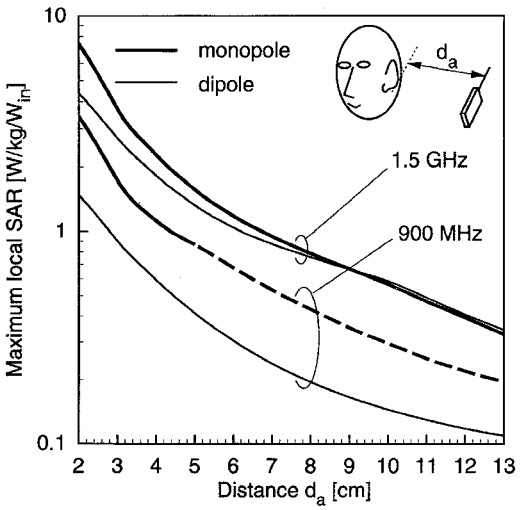

Fig. 6. The calculated maximum local SAR's within any 1 g tissue in the heterogeneous head model versus the distance $\mathbf{d}_a$ between the axis of the antenna and the auricle. The antenna input power is 1 W. The solid line means that the maximum local SAR appears around the auricle. The broken line means that the maximum local SAR appears in the lower part of the cheek.

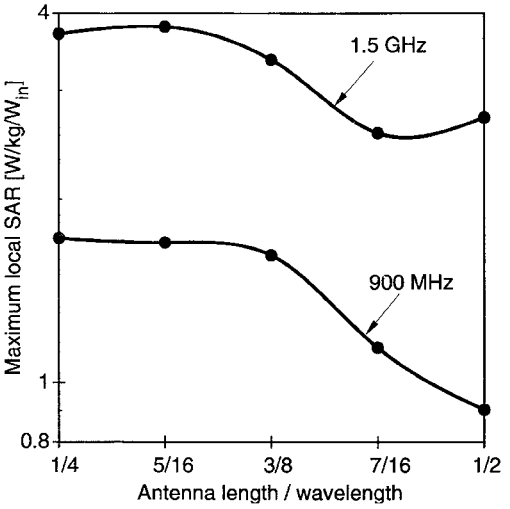

Fig. 7. Calculated maximum local SAR's as a function of antenna length. The antenna input power is 1 W, and the radio models are positioned at the typical location ($\mathbf{d}_a$ = 3 cm).

Fig. 4(a)–(d). In each case, the maximum local SAR occurs in the area behind the left auricle proximate to the radio. No hot spot deep in the head [28] is evident. The power absorption at 1.5 GHz [Fig. 5(c) and (d)] occurs more superficially than does that at 900 MHz [Fig. 5(a) and (b)]. The results agree with the findings in [11], [13]. The absorption in the eyes of the head model is greater for the 1/4-wavelength monopole [Fig. 5(a) and (c)] than for the 1/2-wavelength dipole [Fig. 5(b) and (d)]. For both exposure conditions, however, the maximum local SAR's in the eyes are less than 10% of those in the whole head.

Dependence of the Maximum Local SAR on the Distance: The calculated maximum local SAR's within any 1 g tissue ($4 \times 4 \times 4$ cells) in the heterogeneous head model is plotted in Fig. 6 versus the distance from the left auricle to the axis of the antenna. The hand holding the radio was not considered in calculating the curves plotted here. Maximum local SAR's appear around the auricle except when the 900-MHz 1/4-wavelength monopole antenna is used and the distance $\mathbf{d}_a$ is more than 4 cm. Then they appear in the lower part of the cheek.

The maximum local SAR's at 1.5 GHz are larger than those at 900 MHz, and this difference is due to the difference in the penetration depth. Power at 1.5 GHz is absorbed more superficially than is power at 900 MHz. For the exposure at 900 MHz, the maximum local SAR's are lower when the 1/2-wavelength dipole antenna is used than when the 1/4-wavelength monopole antenna is used. This is because the

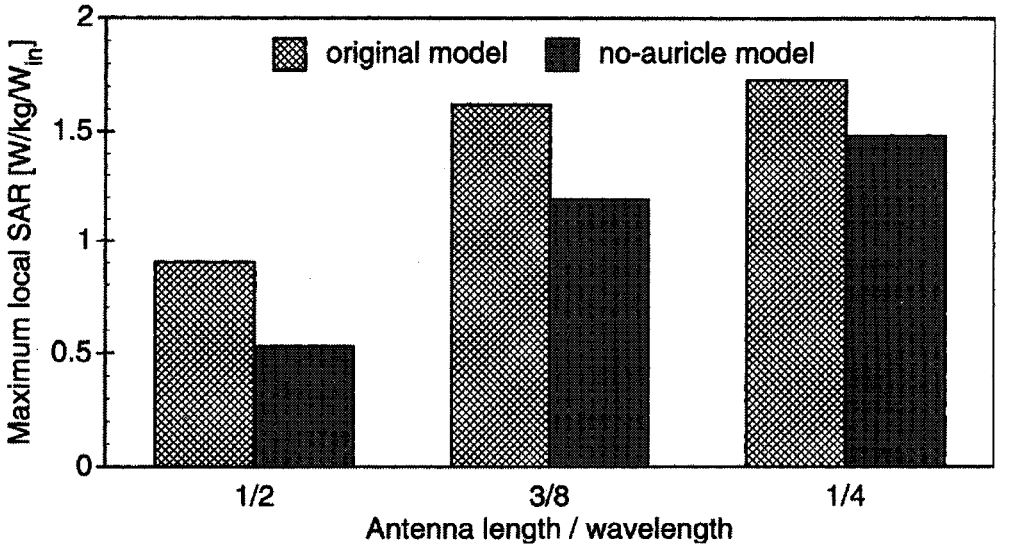

Fig. 8. The calculated maximum local SAR's in the no-auricle head model and those in the original head model. The antenna input power is 1 W. The frequency is 900 MHz. The distance $\mathbf{d}_h$ between the temple of the head model and the antenna axis of the radio model is 4.75 cm (i.e., $\mathbf{d}_a = 3$ cm for the original model).

position of the maximum current on the dipole antenna is farther from the head than is that on the monopole antenna.

Fig. 6 shows that although the location and the absolute value of the maximum local SAR depend on the antenna type and the frequency, the dependences of the maximum local SAR's on the distance $\mathbf{d}_a$ are similar for the various exposure conditions; they all decrease in roughly proportion to $\mathbf{d}_a^{-3/2}$. The distance dependence shown in Fig. 6 is consistent with the results calculated by Dimbylow *et al.* [11].

Effect of Antenna Length on the Maximum Local SAR: In the above calculations, the 1/4-wavelength monopole and the 1/2-wavelength dipole are assumed. However, hand-held portable radios with the whip antenna whose length is between 1/4 and 1/2 of the wavelength are also used [16]. So to investigate the dependence of the maximum local SAR on the antenna length, we also calculated the SAR's in the head exposed to EMF's from the radios with whip antennas with lengths corresponding to 5/16 or 3/8 or 7/16 of the wavelength. Fig. 7 shows the dependence of the maximum local SAR's on antenna lengths from 1/4 to 1/2 of the wavelength. The hand holding the radio was not considered in calculating the curves plotted here. The maximum local SAR's appear around the left auricle regardless of the antenna length between 1/4 and 1/2 of the wavelength.

The maximum local SAR's for the 5/16-wavelength whip and for the 3/8-wavelength whip are comparable to the maximum local SAR for the 1/4-wavelength antenna at both 900 MHz and 1.5 GHz. When the antenna is longer than 3/8 of the wavelength, the maximum local SAR's decrease.

B. Effect of the Auricle on the Maximum Local SAR

As described in the above sections and in [13], the maximum local SAR's appear around the auricle proximate to the radio when the radio is positioned at the typical location in ordinary use. This implies that the maximum local SAR is strongly affected by the auricle.

To investigate the effect of the auricle on the maximum local SAR, we assumed a head model without auricles. The shape of this model is identical to the original model assumed in the above sections except that it has no auricle. The SAR's in the head models with or without auricles were calculated for exposures to EMF's from the radio models with a 1/4-wavelength or 3/8-wavelength monopole antenna or a 1/2-wavelength dipole antenna. Fig. 8 shows a comparison of the maximum local SAR's for the no-auricle model with those for the original model. The hand holding the radio was not considered in calculating the values compared in this figure. It is shown that the maximum local SAR's for the no-auricle model are less than those for the original model and that the effect of the auricle is more remarkable for longer antennas.

C. Effects of the Inhomogeneity of the Head Model

SAR Distribution: Figs. 9 and 10 show the calculated SAR distributions in the homogeneous head model. The exposure conditions for parts (a)–(d) of Figs. 9 and 10 are the same as those for parts (a)–(d) of Figs. 4 and 5. The SAR distributions on the surface of the homogeneous model (Fig. 9) agree well with those on the surface of the heterogeneous model (Fig. 4). On the other hand, the SAR distributions in the horizontal section in the homogeneous model (Fig. 10) differ from those in the heterogeneous model (Fig. 5). The difference is particularly remarkable in the regions corresponding to the tissues of the eye and the bone.

The experimentally measured SAR distributions on the surface of the homogeneous head phantom are shown in Fig. 11. The experimentally measured SAR distribution for the exposure to the EMF from the radio with 1/4-wavelength monopole antenna [Fig. 11(b)] agrees fairly well with the corresponding calculated SAR distributions in the heterogeneous and homogeneous head models exposed by the 1/4-wavelength monopole antenna (Figs. 4(b) and 9(b)). The SAR distribution

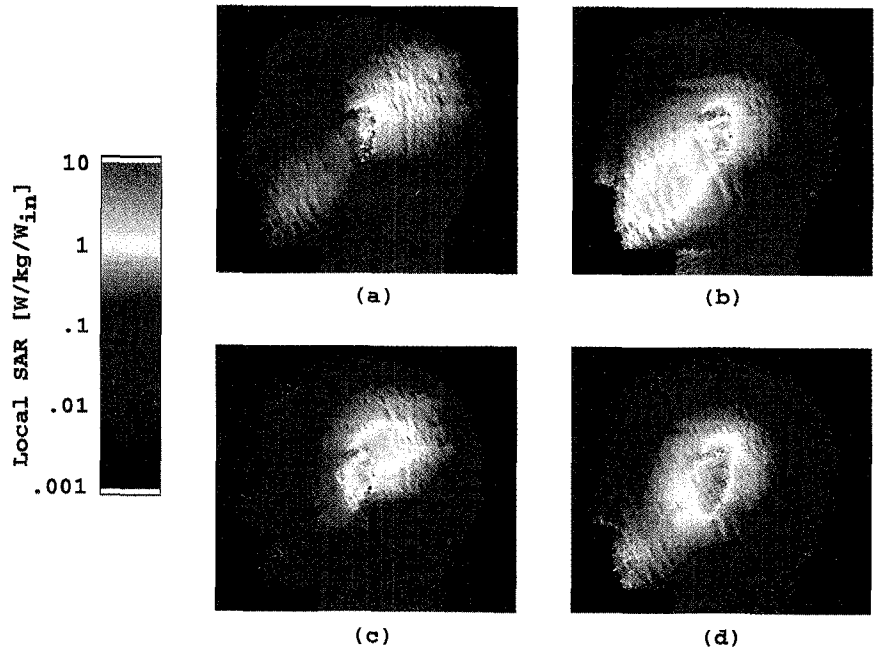

Fig. 9. The calculated SAR distributions on the surface of the homogeneous head model. The exposure conditions are the same as those in Fig. 4.

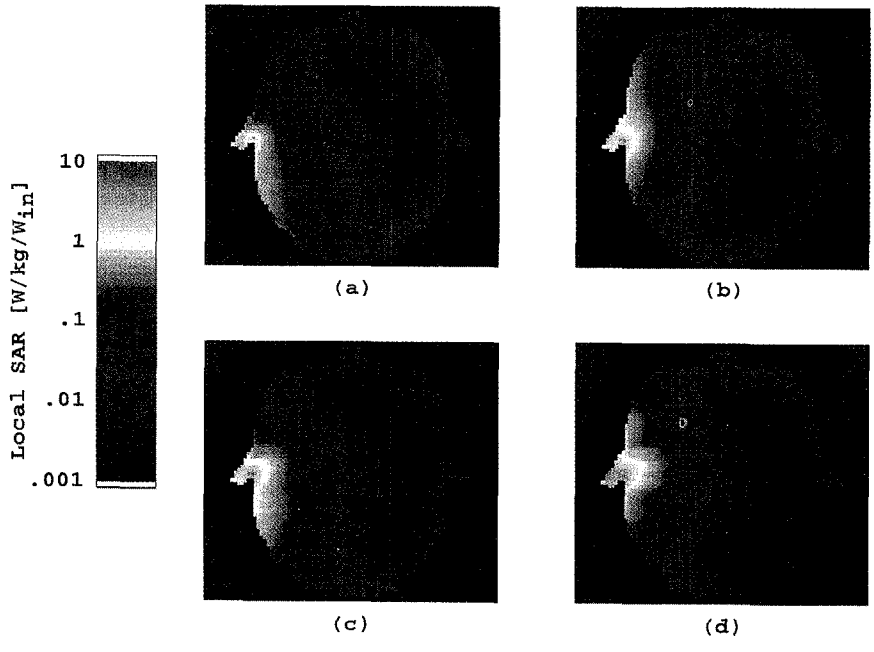

Fig. 10. The calculated SAR distributions in the horizontal section through the eyes of the homogeneous head model. The exposure conditions are the same as those in Fig. 4.

for the radio with the 3/8-wavelength antenna [Fig. 11(a)] is similar to the calculated SAR distributions for the 1/2-wavelength dipole antenna [Figs. 4(a) and 9(a)] even though this antenna length is less than 1/2 of the wavelength.

Maximum Local SAR: The calculated maximum local SAR's in the homogeneous head model and the experimentally measured maximum local SAR's on the surface of the homogeneous head phantom are shown in Fig. 12. For comparison, the calculated maximum local SAR's in the heterogeneous head model (which are the same as those in Fig. 6) are also shown. It should be noted that the experimentally obtained values of local SAR's do not represent the values averaged over 1 g tissue. The absence of this averaging process brings higher SAR values than when the averaging is performed [8].

For the exposure to EMF's from the 1/2-wavelength dipole, the calculated maximum local SAR's in the homogeneous head model agree well with those in the heterogeneous head model. Both in the homogeneous model and the heterogeneous model, the maximum local SAR's appear around the left auricle in this case. It is, therefore, suggested that the maximum local SAR around the auricle proximate to the radio depends not on the inhomogeneity of the head but on the shape of the head and the auricle.

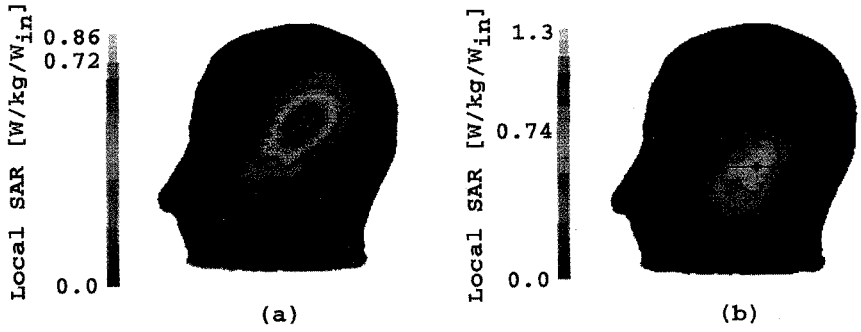

Fig. 11. The experimentally measured SAR distributions on the surface of the homogeneous head phantom exposed to EMF's from radios with either (a) a 3/8-wavelength whip antenna (Radio A) or (b) a 1/4-wavelength whip antenna (Radio D). The antennna input power is 1 W, and the distance between the suface of the conducting box of the radio and the auricle is 1 cm (i.e., $\mathbf{d}_r = 1$ cm). The lengths of the antennas and excitation frequencies are listed in Table II.

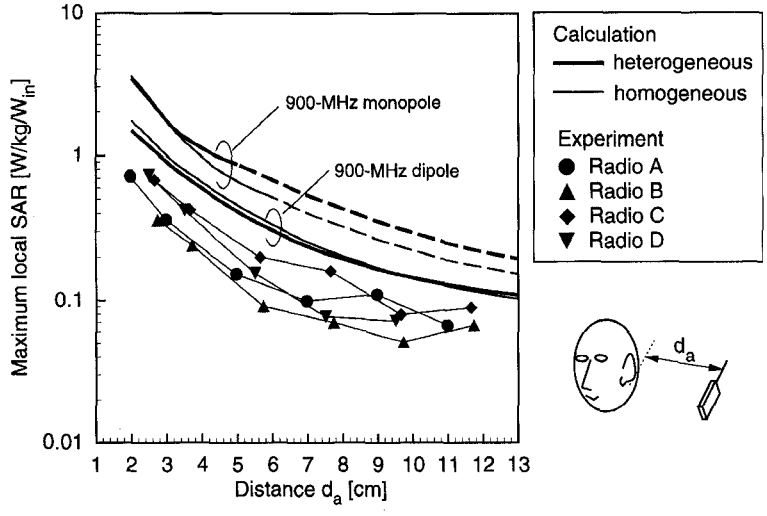

Fig. 12. The numerically calculated maximum local SAR's in the heterogeneous head model and in the homogeneous head model, and the experimentally measured maximum local SAR on the surface of the homogeneous head phantom. The abscissa is the distance $\mathbf{d}_a$. The calculated curves are for radio models operating at 900 MHz. The antenna lengths and frequencies of the radios used in the experiment are listed in Table II. The antenna input power is 1 W. The solid line means that the maximum local SAR appears around the auricle. The broken line means that the maximum local SAR appears in the lower part of the cheek.

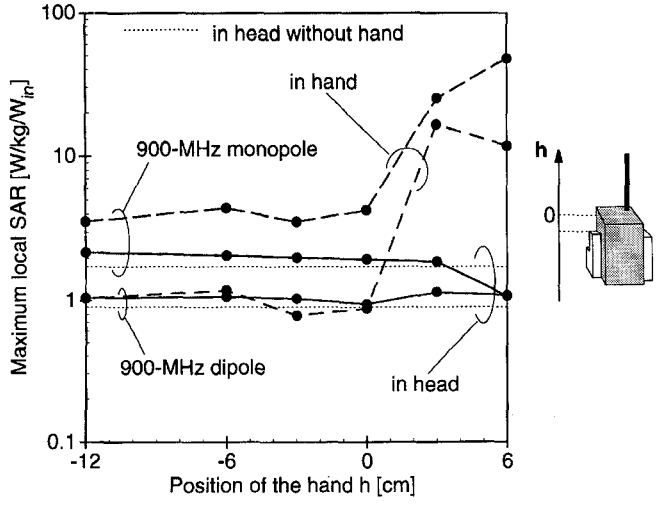

Fig. 13. The calculated maximum local SAR's in the head and in the hand versus the position $\mathbf{h}$ of the hand holding the radio model. The antenna input power is 1 W, the distance $\mathbf{d}_a$ is 3 cm, and the frequency is 900 MHz.

For the exposure to EMF's from the 1/4-wavelength monopole, the difference between the maximum local SAR's calculated for the homogeneous and heterogeneous models is small when the distance between the head and the radio is small ($\mathbf{d}_a \leq 4$ cm). When the distance is larger ($\mathbf{d}_a > 4$ cm), however, the maximum local SAR's in the homogeneous head model are less than those in the heterogeneous head model. In this case, the maximum local SAR in the homogeneous head model appears on the surface of the lower part of the cheek, while that in the heterogeneous head model appears inside the cheek near the oral cavity. This implies that the maximum local SAR in the cheek is dependent on the inhomogeneity.

The experimentally measured maximum local SAR's are much less than the calculated values, although the dependence of the maximum local SAR's on the distance $\mathbf{d}_a$ fairly agrees with the calculation results. This discrepancy between the calculated SAR's and the measured SAR's may be attributed in part to the differences in the head models. For example, the auricles of the head phantom used in the experiment are much smaller than those of the numerical model, and this size difference would, as described in the above section, result in smaller maximum local SAR's. It should also be noted that the power reflected from the antenna is ignored in these calculations (i.e., the calculated SAR represents a worst-case situation). The reflected power, however, is not enough to explain the discrepancy between the calculation and the

experiment. Estimation by FDTD calculation shows that the reflected power attributable to the antenna input impedance change due to the presence of the head does not exceed 20% of the antenna input power even when the radio is in the close vicinity of the head ($\mathbf{d}_a = 2$ cm). Further study is necessary to clarify the reasons for the discrepancy between the calculated results and the experimental results.

D. Effect of the Hand

A hand-held portable radio in practical use is supported by a hand which is not considered in the above sections. To investigate the effect of the hand holding the radio, we calculated the maximum local SAR's within 1 g tissue as a function of the position of the hand holding the radio.

Fig. 13 shows that when the hand does not shade part of the antenna—as is the case in ordinary use ($\mathbf{h} < 0$)—the maximum local SAR's in the head are nearly constant regardless of the hand position $\mathbf{h}$ and are slightly larger than those in the case where the hand holding the radio is not considered. For the exposure to EMF's from the 1/4-wavelength monopole the maximum local SAR's in the hand are larger than those in the head, while for the 1/2-wavelength dipole the maximum local SAR's in the hand are similar to those in the head.

When the hand shades part of the antenna ($\mathbf{h} > 0$), the maximum local SAR's in the hand critically increase ten times those in the head, although this position of the hand is not where the hand is during ordinary use.

V. Conclusion

Characteristics of the SAR distributions in a head exposed to EMF's from hand-held portable radios operated at 900 MHz and 1.5 GHz were investigated. The SAR distributions in the head were calculated, by the FDTD method, using a heterogeneous and realistic model of a human head as well as a realistic model of a hand-held portable radio. The major findings are summarized as follows:

1) The maximum local SAR decreases roughly in proportion to $\mathbf{d}_a^{-3/2}$ regardless of whether the antenna is a 1/2-wavelength dipole or a 1/4-wavelength monopole and regardless of whether the frequency is 900 MHz or 1.5 GHz.
2) The maximum local SAR decreases with increasing antenna length from 1/4 to 1/2 of the wavelength.
3) The maximum local SAR is lower in for a head model without auricles than for one with auricles.
4) When the radio is located in the vicinity of the head, the maximum local SAR's in the homogeneous head model agree well with those in the heterogeneous model.
5) The maximum local SAR's in the head do not depend on the position of the hand holding the radio as long as the hand does not shade the antenna.

The SAR distributions on the surface of a homogeneous head phantom exposed to EMF's from several types of hand-held portable radios were also measured experimentally by using the thermograph method. Although the experimentally measured SAR distributions on the surface of the head phantom and their dependence on the distance between the head and the radio agreed fairly with the calculated results, the maximum local SAR's obtained experimentally were significantly less than those calculated numerically.

Acknowledgment

The authors wish thank to Mr. Kuramoto, the Executive Manager of NTT DoCoMo, for his useful suggestions in the course of this work.

References

[1] *IEEE Standard for Safety Levels with Respect to Human Exposure to Radio Frequency Electromagnetic Fields 3 kHz to 300 GHz*, IEEE C95.1-1991, Apr. 1992.
[2] "A report of telecommunications technology council for the minsistry of posts and telecommunications," no. 38, *Radio Frequency Protection Guidelines*, Tokyo. RCR Inc., June 1990.
[3] Q. Balzano, O. Garay, and F. R. Steel, "Heating of biological tissue in the induction field of VHF portable radio transmitters," *IEEE Trans. Veh. Technol.*, vol. VT-27, pp. 51–56, May 1978.
[4] Q. Balzano, O. Garay, and F. R. Steel, "Energy deposition in simulated human operators of 800-MHz portable transmitters," *IEEE Trans. Veh. Technol.*, vol. VT-27, pp. 174–181, Nov. 1978.
[5] I. Chatterjee, Y.-G Gu, and O. P. Gandhi, "Quantification of electromagnetic absorption in humans from body-mounted communication transceivers," *IEEE Trans. Veh. Technol.*, vol. VT-34, pp 55–62, May 1985.
[6] R. F. Cleveland Jr. and T. W. Athey, "Specific absorption rate (SAR) in models of the human head exposed to hand-held UHF portable radios," *Bioelectromagn.*, vol. 10, pp. 173–186, 1989.
[7] T. Kobayashi, T. Nojima, K. Yamada, and S. Uebayashi, "Dry phantom composed of ceramics and its application fo SAR estimation," *IEEE Trans. Microwave Theory Tech.*, vol. 41, pp. 136–140, Jan. 1993.
[8] T. Nojima, S. Nishiki, and T. Kobayashi, "An experimental SAR estimation of human head exposed to UHF near field using dry-phantom models and a thermograph," *IEICE Trans. Commun.*, vol. E77-B, pp. 708–713, June 1994
[9] V. Anderson and K. H. Joyner, "Specific absorption rate levels measured in a phantom head exposed to radio frequency transmissions from analog hand-held mobile phones," *Bioelectromagn.*, vol 16, pp. 60–69, 1995.
[10] P J. Dimbylow, "FDTD calculations of the SAR for a dipole closely coupled to the head at 900 MHz and 1.9 GHz," *Phys. Med. Biol.*, vol. 38, pp. 361–368, 1993.
[11] P. J. Dimbylow, "SAR calculations in an anatomically realistic model of the head for mobile communication transceivers at 900 MHz and 1.8 GHz," *Phys. Med. Biol.*, vol. 39, pp. 1537–1553, 1994.
[12] M. A. Jensen and Y. Rahmat-Samii, "EM interaction of handsed antennas and a human in personal communications," *Proc. IEEE*, vol. 83, pp. 7–17, Jan. 1995.
[13] O. P. Gandhi, "Some numerical methods for dosimetry: Extremely low frequencies to microwave frequnecies," *Radio Sci.*, vol. 30, pp. 161–177, Jan.–Feb. 1995.
[14] L. Martens, J. D. Moerloose, D. D. Zutter, J. D. Poorter, and C. D. Wagter, "Calculation of the elelctromagnetic fields induced in the head of an operator of a cordless telephone," *Radio Sci.*, vol. 30, pp. 283–290, Jan –Feb. 1995.
[15] J. Toftgård, S. N. Hornsleth, and J. B. Andersen, "Effects on portable antennas of the presence of a person," *IEEE Trans. Antennas Propagat.*, vol. 41, pp. 739–746, June 1993.
[16] Y. Yamada, N. Terada, K. Tsunekawa, and H. Itakura, "The technology of antennas for mobile communications," *NTT DoCoMo Technical Journal*, vol. 1, pp. 37–43, Jan. 1994.
[17] H.-Y. Chen and H.-H. Wang, "Current and SAR induced in a human head model by the electromagnetic fields irradiated from a cellular phone," *IEEE Trans. Microwave Theory Tech.*, vol. 42, pp. 2249–2254, Dec. 1994.
[18] O. Fujiwara and A. Kato, "Computation of sar inside eyeball for 1 5-GHz microwave exposure using finite-difference time-domain technique," *IEICE Trans. Commun.*, vol. E77-B, pp. 732–737, June 1994.
[19] C. Polk and E. Postow, Eds., *CRC Handbook of Biological Effects of Electromagnetic Fields*. Boca Raton, FL: CRC, 1988
[20] A. Taflove and M. E. Brodwin, "Computation of the electromagnetic fields and induced temperatures within a model of the microwave-irradiated human eye," *IEEE Trans. Microwave Theory Tech.*, vol. MTT-23, pp. 806–888, Nov. 1975.

[21] C. H. Durney, C. C. Johnson, P. W. Barber, H. Massoudi, M. F. Iskander, J. L. Lords, D. K. Ryser, S. J. Allen, and J. C. Mitchel, "Radiofrequency radiation dosimetry handbook," 2nd ed., USAF School of Aerospace Medicine, Brooks Air Force Bace, TX 78235, Tech. Rep. SAM-TR-78-22, 1978.
[22] S. Watanabe, T. Tanaka, and M. Taki, "Effects of the body on the sar distribution in the head of a human model exposed to the near field of a small radiation source and to the far field of the source," in *Proc. Convention Rec. IEICE Japan*, IEICE, Mar. 1995, p. B-241.
[23] K. S. Yee, "Numerical solutions of initial boundary value problems involving Maxwell's equations in isotropic media," *IEEE Trans. Antennas Propagat.*, vol. AP-14, pp. 302–307, May 1966.
[24] A. Taflove and M. E. Brodwin, "Numerical solution of steady-state electromagnetic scattering problems using the time-dependent Maxwell's equations," *IEEE Trans. Microwave Theory Tech.*, vol. MTT-23, pp. 623–630, Aug. 1975.
[25] D. M. Sullivan, D. T. Borup, and O. P. Gandhi, "Use of the finite-difference time-domain method in calculating EM absorption in human tissues," *IEEE Trans. Biomed. Eng.*, vol. BME-34, pp. 148–157, Feb. 1987.
[26] G. Mur, "Absorption boundary conditions for the finite-difference approximation of the time-domain electromagnetic-field equation," *IEEE Trans. Electromagn. Compat.*, vol. EMC-23, pp. 377–382, Nov. 1981.
[27] A. Taflove, K. R. Umashankar, B. Beker, F. Harfoush, and K. S. Yee, "Detailed FD-TD analysis of electromagnetic fields penetrating narrow slots and lapped joints in thick conducting screens," *IEEE Trans. Antennas Propagat.*, vol. 36, pp. 247–257, Feb. 1988.
[28] H. N. Kritikos and H. P. Schwan, "Hot spot generated in conducting spheres by electromagnetic waves and biological implication," *IEEE Trans. Biomed. Eng.*, vol. BME-19, pp. 53–58, Jan. 1972.

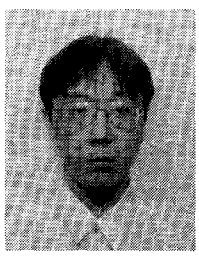

So-ichi Watanabe (S'94) received the B.E., M.E., and Ph.D. degrees in electrical engineering from Tokyo Metropolitan University, Japan, in 1991, 1993, and 1996, respectively.

He is currently with the Communications Research Laboratory of the Ministry of Posts and Telecommunications. His main interests have been biological effects of electromagnetic fields.

Dr. Watanabe is a member of the Institute of Electronics, Information and Communication Engineers of Japan (IEICE).

Masao Taki was born in Tokyo in 1953. He received the B.E. degree from the University of Tokyo in 1976. From 1976 to 1981 he was with the Institute of Medical Electronics, Faculty of Medicine, University of Tokyo as a graduate student. He received the M.E. and the Ph.D. degrees in electronic engineering in 1978 and 1981, respectively, from the University of Tokyo.

He is currently an Associate Professor in the Department of Electronics and Information Engineering, Tokyo Metropolitan University. He has been engaged in the researches on biological effects of electromagnetic fields and noise control engineering.

Dr. Taki is a member of the Institute of Electronics, Information and Communication Engineers of Japan (IEICE), the Japan Society of Medical and Biological Engineering, the Acoustical Society of Japan, and the Institute of Noise Control Engineering of Japan.

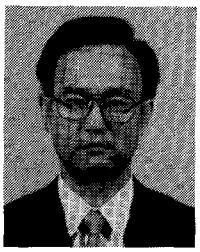

Toshio Nojima (S'72–M'74) received the B.E. degree in electrical engineering from Saitama University in 1972, and the M.E. and Ph.D. degrees in electrical engineering in 1974 and 1988, respectively, from Hokkaido University.

From 1974 to 1992 he was with the Nippon Telegraph and Telephone (NTT) Communication Laboratories, where he was engaged in the development of a high capacity 6-GHz band SSB-AM system and mobile radio systems. Since 1992 he has been with the NTT Mobile Communications Network Inc., where he is currently an Executive Research Engineer. He is now doing research on RF technologies including EMC for mobile radio systems.

Dr. Nojima is a member of the Institute of Electronics, Information and Communication Engineers of Japan (IEICE).

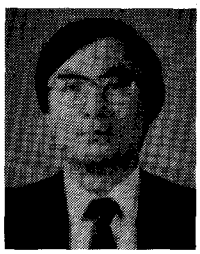

Osamu Fujiwara (M'83) was born in Osaka in 1948. He received the B.E. degree in electronic engineering from the Nagoya Institute of Technology, Nagoya, Japan, in 1971, and the M.E. and the D.E. degrees in electrical engineering from the Nagoya University, Nagoya, Japan, in 1973 and in 1980, respectively.

From 1973 to 1976, he worked in the Central Research Laboratory, Hitachi, Ltd., Kokubunji, Japan, where he was engaged in research and development on system packaging designs for computers. From 1980 to 1984 he was with the Department of Electrical Engineering at the Nagoya University. In 1984 he moved to the Department of Electrical and Computer Engineering at the Nagoya Institute of Technology, where he is presently a Professor. His research interests include measurements of electromagnetic environment, bioelectromagnetics and other related areas of electromagnetic compatibility (EMC).

Dr. Fujiwara is a member of the Institute of Electronics, Information and Communication Engineers of Japan (IEICE) and of the Institute of Electrical Engineers of Japan (IEE). He is an Associate Editor for the IEICE Transactions on Communications and for the IEEE TRANSACTIONS ON ELECTROMAGNETIC COMPATIBILITY.